

A configuration interaction correction on top of pair coupled cluster doubles

Artur Nowak¹ and Katharina Boguslawski^{1, a)}

Institute of Physics, Faculty of Physics, Astronomy and Informatics, Nicolaus Copernicus University in Toruń, Grudziadzka 5, 87-100 Toruń, Poland

(Dated: 3 November 2022)

Numerous numerical studies have shown that geminal-based methods are a promising direction to model strongly correlated systems with low computational costs. Several strategies have been introduced to capture the missing dynamical correlation effects, which typically exploit *a posteriori* corrections to account for correlation effects associated with broken-pair states or inter-geminal correlations. In this article, we scrutinize the accuracy of the pair coupled cluster doubles (pCCD) method extended by configuration interaction (CI) theory. Specifically, we benchmark various CI models, including, at most double excitations against selected CC corrections as well as conventional single-reference CC methods. A simple Davidson correction is also tested. The accuracy of the proposed pCCD-CI approaches is assessed for challenging small model systems such as the N₂ and F₂ dimers and various di- and triatomic actinide-containing compounds. In general, the proposed CI methods considerably improve spectroscopic constants compared to the conventional CCSD approach, provided a Davidson correction is included in the theoretical model. At the same time, their accuracy lies between the linearized frozen pCCD and frozen pCCD variants.

I. INTRODUCTION

The reliable and efficient description of electron correlation effects is an open problem in quantum chemistry. Although the correlation energy is quantitatively small compared to the total electronic energy, the proper description of the correlated motion of the electrons is crucial to understand physical and chemical phenomena like bond-breaking processes. Typically, electron correlation effects are divided into a dynamical and a non-dynamical/static part. To capture both contributions simultaneously, we require advanced methods that exploit a multireference description. Examples thereof are multireference coupled cluster approaches,^{1–3} the density matrix renormalization group (DMRG) algorithm,^{4–16} or quantum Monte Carlo methods.^{17,18} Despite their high accuracy, these methods are computationally rather expensive.

An alternative strategy to account for strong electron correlation effects is to exploit geminal-based methods.¹⁹ The key idea of geminal-based electronic structure approaches is to use non-interacting electron pairs as the fundamental building blocks of the electronic wave function. Various numerical studies using geminal-based methods, such as the anti-symmetric product of interacting geminals,^{20–25} the antisymmetric product of strongly orthogonal geminals (APSG),^{26–36} singlet-type strongly orthogonal geminals,^{37–39} geminals constructed from Richardson–Gaudin states,^{40–44} and the antisymmetric product of 1-reference orbital geminals,^{45,46} also known as the pair-coupled cluster doubles (pCCD) ansatz,⁴⁷ yield promising results. Specifically, the pCCD approach is a product of geminal creation operators ϕ_i^\dagger acting on some vacuum state

$$|\text{pCCD}\rangle = \prod_{i=1}^P \phi_i^\dagger |0\rangle, \quad (1)$$

with P being the number of electron pairs and

$$\phi_i^\dagger = a_i^\dagger a_{\bar{i}}^\dagger + \sum_a^{\text{virt}} c_i^a a_a^\dagger a_{\bar{a}}^\dagger, \quad (2)$$

where the sum runs over all virtual orbitals a and $\{c_i^a\}$ are the geminal expansion coefficients. In eq. (2), i (\bar{i}) indicates spin-up (spin-down) electrons. Using an exponential ansatz,⁴⁵ the pCCD wave function can be rewritten as

$$\begin{aligned} |\text{pCCD}\rangle &= \exp\left(\sum_i^{\text{occ}} \sum_a^{\text{virt}} c_i^a a_a^\dagger a_{\bar{a}}^\dagger a_i\right) |\Phi_0\rangle \\ &= \exp(\hat{T}_p) |\Phi_0\rangle, \end{aligned} \quad (3)$$

where $|\Phi_0\rangle$ is some independent-particle wave function, for instance, the Hartree–Fock (HF) determinant, and \hat{T}_p is the electron-pair cluster operator. One benefit in using the exponential form is the proper (linear) scaling of the method with the number of electrons (size-extensivity). To recover size-consistency it is necessary to apply an orbital-optimization protocol^{46–49} which also leads to localized orbitals, which are symmetry-broken.^{46–49} Investigations on the one-dimensional Hubbard model^{46,50} or molecules with stretched bonds,^{47,51–60} even those containing lanthanide⁶¹ or actinide atoms^{55,56,62} demonstrate that geminal-based approaches can capture an important part of static/nondynamic electron correlation effects. Since pCCD requires a reasonable amount of computational resources (with a scaling of N^4 or N^3 if proper intermediates are defined), heavy-element-containing compounds are a promising scope of applications.⁶³ Nevertheless, by restricting the wave function ansatz to electron-pair states, a large fraction of the correlation energy is not accounted for. This missing dynamical electron correlation energy that cannot be described using electron-pair states, is commonly included *a posteriori* by means of, for instance, perturbation theory,^{58,64–66} a coupled cluster ansatz,^{52,57,67,68} or density functional approximations.^{69,70} In this work, we develop a different *a posteriori* correction for a pCCD reference function using configuration interaction (CI) theory. Specifically,

^{a)}Electronic mail: k.boguslawski@fizyka.umk.pl

we will focus on a CI correction, which is restricted to hole-particle excitations with respect to a reference determinant. Similar CI models have been already combined with, for instance, an APSG,⁷¹ generalized valence bond,^{72–75} or an anti-symmetrized geminal power⁷⁶ reference function.

This work is organized as follows. In section II, we briefly summarize the theory of the CI corrections on top of pCCD, which are introduced using a spin-free formalism. The computational details are summarized in section III, while the numerical results are presented in sections IV–V. Finally, we conclude in section VI.

II. CI CORRECTIONS WITH A PCCD REFERENCE FUNCTION

Conventional (truncated) CI methods define the electronic wave function as a linear combination of all possible “excited” configurations with respect to some reference configuration $|\Phi_0\rangle$,

$$|\text{CI}\rangle = \sum_{\mu} c_{\mu} \hat{\tau}_{\mu} |\Phi_0\rangle = \sum_{\mu} c_{\mu} |\Phi_{\mu}\rangle, \quad (4)$$

where in this compact representation c_{μ} are the CI coefficients and $\hat{\tau}_{\mu}$ is an excitation operator including occupied–virtual (or hole–particle) excitations up to a predefined level. To arrive at a CI-type correction, we replace the reference determinant with a pCCD reference function eq. (3),

$$|\text{pCCD-CI}\rangle = \sum_{\mu} c_{\mu} \hat{\tau}_{\mu} e^{\hat{T}_p} |\Phi_0\rangle. \quad (5)$$

Substituting this ansatz for the electronic wave function $|\Psi\rangle$ in the Schrödinger equation $\hat{H}|\Psi\rangle = E|\Psi\rangle$, we obtain

$$\begin{aligned} \sum_{\mu} \hat{H} c_{\mu} \hat{\tau}_{\mu} e^{\hat{T}_p} |\Phi_0\rangle &= E \sum_{\mu} c_{\mu} \hat{\tau}_{\mu} e^{\hat{T}_p} |\Phi_0\rangle \\ \sum_{\mu} \hat{H} e^{\hat{T}_p} c_{\mu} \hat{\tau}_{\mu} |\Phi_0\rangle &= E \sum_{\mu} e^{\hat{T}_p} c_{\mu} \hat{\tau}_{\mu} |\Phi_0\rangle \end{aligned} \quad (6)$$

where \hat{H} is the electronic Hamiltonian comprising one- and two-electron integrals and we utilized that $\hat{\tau}_{\mu}$ and \hat{T}_p commute as they contain only hole–particle excitation operators, $[\hat{\tau}_{\mu}, \hat{T}_p] = 0$. Unfortunately, the eigenvalue problem of eq. (6) cannot be solved in its symmetric representation as the corresponding series expansion, that enters the working equation, does not truncate. In order to solve for the eigenvalues and eigenvectors efficiently, we can project out the components of interests, which will lead to a diagonalization problem of a non-Hermitian matrix. There are several choices for the projection space, which is defined in terms of the de-excitation operator $\hat{\tau}_{\mu}^{\dagger}$. We can either project by $\langle\Phi_0|\hat{\tau}_{\mu}^{\dagger}$ or $\langle\Phi_0|\hat{\tau}_{\mu}^{\dagger} e^{-\hat{T}_p}$. We should note that if we restrict the CI operator to comprise at most single and double excitations, both projection schemes will result in the same solutions.⁷¹ In the following, we will focus on the latter approach. Multiplying eq. (6) from left with $e^{-\hat{T}_p}$ and using the property that \hat{T}_p and $\hat{\tau}_{\mu}$ commute, results

in

$$\begin{aligned} e^{-\hat{T}_p} \hat{H} e^{\hat{T}_p} \sum_{\mu} c_{\mu} \hat{\tau}_{\mu} |\Phi_0\rangle &= E \sum_{\mu} c_{\mu} \hat{\tau}_{\mu} e^{-\hat{T}_p} e^{\hat{T}_p} |\Phi_0\rangle \\ \mathcal{H}^{(p)} \sum_{\mu} c_{\mu} \hat{\tau}_{\mu} |\Phi_0\rangle &= E \sum_{\mu} c_{\mu} \hat{\tau}_{\mu} |\Phi_0\rangle. \end{aligned} \quad (7)$$

Thus, the complex CI problem has now the form of a conventional single-reference (truncated) CI model, where the Hamiltonian is substituted by the similarity-transformed Hamiltonian of pCCD $\mathcal{H}^{(p)}$. The diagonalization problem becomes computationally feasible and can be solved in efficient time as the commutator expansion of $e^{-\hat{T}_p} \hat{H} e^{\hat{T}_p}$ naturally truncates. The corresponding working equations bear similarities to the EOM formalism^{77–80} as EOM-CC diagonalizes the similarity-transformed Hamiltonian of a given CC model. The main difference between conventional EOM-CC and the proposed pCCD-CI model is that the similarity-transformed Hamiltonian to be diagonalized has a particular simple form (as it only accounts for electron-pair excitation), while the CI ansatz includes any choice for the excitation operator. In standard EOM-CC theory, both the CC cluster operator and the CI ansatz are restricted to the same order of excitations.

Furthermore, we will consider only singlet excitations. The corresponding projection manifold will result in a spin-free CI problem, where all eigenstates of $\mathcal{H}^{(p)}$ will be singlet states. Moreover, from all working equations, we have subtracted the energy of the reference function, that is, the pCCD total energy (similar to the conventional CI equations, where the energy of the reference determinant is subtracted). Thus, the eigenenergies correspond to excitation energies with respect to the pCCD reference function. In this spin-free formulation, the excitation operator that contains single excitations can be expressed as follows

$$\begin{aligned} \hat{\tau} &= \hat{\tau}_0 + \hat{\tau}_S = c_0 + \sum_{ia} c_i^a (a_a^{\dagger} a_i + a_a^{\dagger} a_i^{\dagger}) \\ &= c_0 + \sum_{ia} c_i^a E_i^a, \end{aligned} \quad (8)$$

where we introduced the singlet one-electron excitation operator $E_i^a = a_a^{\dagger} a_i + a_a^{\dagger} a_i^{\dagger}$. To account for double excitations, the above operator is modified as follows

$$\begin{aligned} \hat{\tau} &= \hat{\tau}_0 + \hat{\tau}_D \\ &= c_0 + \frac{1}{2} \sum_{ijab} c_{ij}^{ab} (a_a^{\dagger} a_b^{\dagger} a_j a_i + a_a^{\dagger} a_b^{\dagger} a_j^{\dagger} a_i + a_a^{\dagger} a_b^{\dagger} a_j a_i^{\dagger} + a_a^{\dagger} a_b^{\dagger} a_j^{\dagger} a_i^{\dagger}) \\ &= c_0 + \frac{1}{2} \sum_{ijab} c_{ij}^{ab} E_i^a E_j^b. \end{aligned} \quad (9)$$

To arrive at a CISD correction, the excitation operators for singles and doubles are combined, that is, $\hat{\tau} = \hat{\tau}_0 + \hat{\tau}_S + \hat{\tau}_D$. We should note that we tested two different $\hat{\tau}_D$ excitation operators. In the pCCD-CID and pCCD-CISD model, all electron pair excitations are excluded from the CI ansatz as they are already accounted for in the pCCD reference calculations. If we are interested in targeting several roots, that is, the electronic ground state and some lowest-lying electronically excited states, this approximation will neglect any double excitations of electron-pair character and, hence, bi-excited states

might miss important contributions to the wave function expansion. Thus, in the pCCD-CID' and pCCD-CISD' models, the electron-pair sector is added to the general excitation operator $\hat{\tau}_D$. However, including electron-pair excitations in the CI ansatz might lead to double-counting problems of electron correlation effects associated with electron-pair states. In the following, we assess both CI ansätze (with and without electron-pair excitations) in describing ground and electronically excited states.

In order to solve eq. (7), that is, to find the eigenvalues and eigenvectors of $\mathcal{H}^{(p)}$, its matrix representation has to be diagonalized. In practical calculations, iterative techniques are used to compute only a few of the lowest eigenvalues and corresponding eigenvectors, for instance non-Hermitian extensions of the Davidson algorithm (the corresponding working equations are collected in the SI). We should note that the projection manifold has a special form⁸¹ (similar to spin-free CC theory) to allow for an algebraic spin summation, which results in the spin-free pCCD-CI working equations,

$$\langle \Phi_I^A | = \frac{1}{2} \langle \Phi_0 | E_a^i \quad (10)$$

$$\langle \Phi_{IJ}^{AB} | = \frac{1}{3} \langle \Phi_0 | E_b^j E_a^i + \frac{1}{6} \langle \Phi_0 | E_a^j E_b^i. \quad (11)$$

Finally, we include a Davidson correction on top of the proposed pCCD-CI models to minimize the size-consistency error intrinsic to (truncated) CI methods.^{82,83} Specifically, we combine a renormalized Davidson correction introduced in Ref. 84 exploiting the pCCD-CI correlation energy,

$$E_{\text{RDC}} = \left(\frac{1 - c_0^2}{c_0^2} \right) (E_{\text{pCCD-CI}} - E_{\text{RF}}), \quad (12)$$

where $E_{\text{pCCD-CI}}$ indicates the total energy of the pCCD-CI method, E_{RF} is the energy of the reference method (here pCCD), and c_0 is the contribution of the reference determinant ($|\Phi_0\rangle$) of the reference method.

III. COMPUTATIONAL DETAILS

A. Basis sets, relativistic effects, and frozen core

For the light diatomic molecules H_2 and N_2 , we used the triple- ζ correlation consistent basis sets of Dunning⁸⁵ (cc-pVTZ), while for F_2 the augmented version (aug-cc-pVTZ) was employed. For all actinide compounds, we used the double- ζ correlation consistent basis sets of Peterson⁸⁶ (cc-pVDZ-DK3) for all heavy elements, optimized specifically for the DKH3 Hamiltonian,⁸⁷⁻⁹⁰ and Dunning's aug-cc-pVDZ basis set for all the remaining light elements. Scalar relativistic effects were accounted for by the DKH3 Hamiltonian. All calculations for systems containing heavy-elements were performed with a frozen core to ensure a compromise between computational efficiency, the reliability of the results for heavy-element-containing systems, and the quality of the atomic basis sets.^{55,91-93} Specifically, the atomic 1s orbitals of the O and N atom, the 1s, 2s, and 2p orbitals of the S atom,

and up to the 5d orbitals of the Th, Pa, and U center were frozen. All post-pCCD methods as well as all CCD and CCSD calculations were performed using a developer version of the PYBEST v1.2.0 software package.⁹⁴⁻⁹⁶ All pCCD-based calculations exploited the natural orbitals obtained from orbital-optimized pCCD, while all conventional CC calculations featured canonical Hartree-Fock orbitals. The CCSD(T) reference calculations were performed in the MOLPRO2020⁹⁷ software suite.

B. Evaluations of spectroscopic constants

The potential energy curves were obtained from a polynomial fit of 8-th order using the fitting scripts available in the PYBEST⁹⁵ software package. From these fitted potential energy curves, we derived the corresponding spectroscopic constants such as equilibrium bond lengths (r_e) and harmonic vibrational frequencies (ω_e) for all actinide compounds and light diatomic molecules. Additionally, the potential energy well depths (D_e) were calculated from fitting a generalized Morse function. To determine the harmonic vibrational frequencies (ω_e), we performed numerical calculations using the five-point finite difference stencil⁹⁸ with the following averaged masses: uranium: 238.0508, thorium: 232.0381, protactinium: 231.0359, oxygen: 15.9949, sulfur: 31.9721, and nitrogen: 14.0031.⁹⁹

IV. ASSESSING THE ACCURACY OF THE CI CORRECTIONS FOR LIGHT DIATOMIC MOLECULES

Our first test set to assess the performance of the CI corrections contains the N_2 and F_2 diatomic molecules. In these systems, the different flavors of electron correlation effects are difficult to describe with various pCCD corrections. For instance, a remarkable challenging problem for computational chemistry is to accurately model the electronic structure of the N_2 molecule^{52,68,100-103} along its dissociation pathway. This problem is related to dynamic changes in the contributions of electron correlation effects for an increasing interatomic distance. In general, around the equilibrium distances, dynamical electron correlation effects are prevalent, while the contribution of nondynamic/static electron correlation significantly increases when the N-N bond is stretched. Furthermore, all CC corrections on top of pCCD restricted to at most double excitations fail and do not yield a physically meaningful dissociation limit. Unlike in the nitrogen dimer, dynamical correlation effects are dominant in the F_2 molecule. Conventional methods require even triple excitations to model the dissociation pathway of F_2 reliably.^{68,102-104} Thus, the F_2 dimer represents a good test system to assess if novel methods can accurately describe a bond-breaking process without increasing the computational cost related to the inclusion of triple (or higher) excitations. Since pCCD-based methods do not provide sufficiently accurate results in these systems, they represent a good testing ground to assess the accuracy and robustness of the CI corrections.

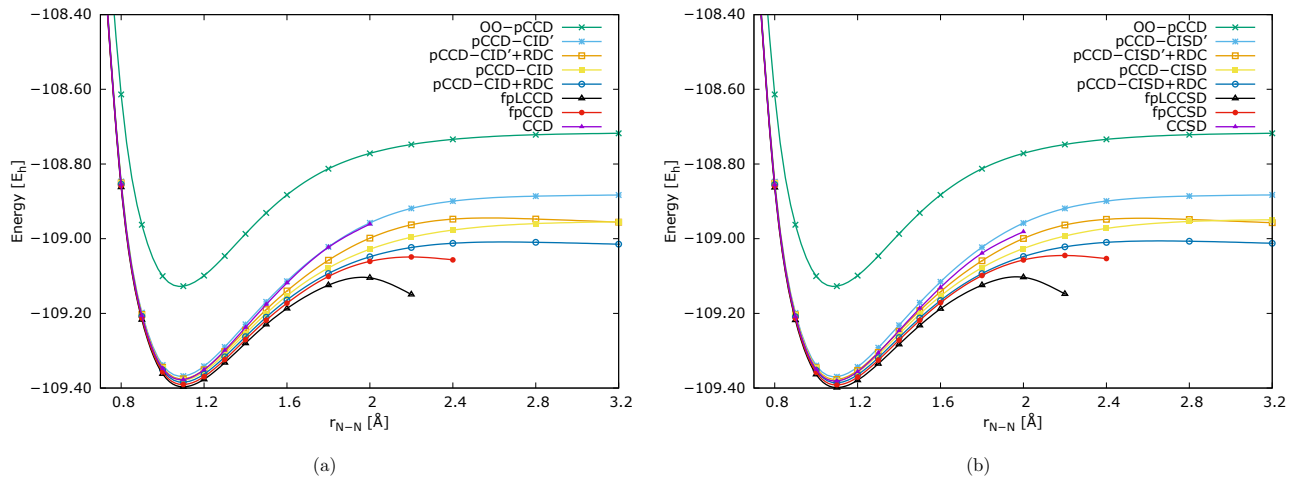


FIG. 1. Potential energy surfaces of the ground states of N_2 determined for various post-pCCD with (a) doubles excitation and (b) singles and doubles excitations. The superscript ' indicates that the CI operator also includes the electron pair sector. RDC: renormalized Davidson correction.

TABLE I. Spectroscopic parameters for the ground state of the N_2 molecule obtained from various post-pCCD methods and conventional CC models. r_e is the equilibrium bond length, ω_e the harmonic vibrational frequency, and D_e the dissociation energy, respectively. The differences with respect to experimental result Δ_{exp} or MRCI reference data Δ_{MRCI} are given in parentheses. The total electronic energies are summarized in the SI. RDC: renormalized Davidson correction.

Method	r_e [Å]	Δ_{MRCI}	Δ_{exp}	ω_e [cm^{-1}]	Δ_{MRCI}	Δ_{exp}	D_e [$\frac{\text{kcal}}{\text{mol}}$]	Δ_{MRCI}	Δ_{exp}
oo-pCCD	1.085	(-0.019)	(-0.013)	2517	(+176)	(+158)	244.8	(+26.9)	(+19.7)
pCCD-CID'	1.091	(-0.013)	(-0.007)	2454	(+113)	(+95)	304.3	(+86.4)	(+79.2)
pCCD-CID'+RDC	1.095	(-0.009)	(-0.003)	2407	(+66)	(+48)	263.3	(+45.4)	(+38.2)
pCCD-CID	1.096	(-0.008)	(-0.002)	2399	(+58)	(+40)	266.1	(+48.2)	(+41.0)
pCCD-CID+RDC	1.099	(-0.005)	(+0.001)	2369	(+28)	(+10)	231.9	(+14.0)	(+6.8)
fpLCCD	1.101	(-0.003)	(+0.003)	2347	(+6)	(-12)			
fpCCD	1.100	(-0.004)	(+0.002)	2365	(+24)	(+6)			
CCD	1.093	(-0.011)	(-0.005)	2447	(+106)	(+88)			
pCCD-CISD'	1.088	(-0.016)	(-0.013)	2447	(+106)	(+88)	305.4	(+87.5)	(+80.3)
pCCD-CISD'+RDC	1.095	(-0.009)	(-0.003)	2396	(+55)	(+37)	263.3	(+45.4)	(+19.7)
pCCD-CISD	1.097	(-0.007)	(-0.001)	2394	(+53)	(+35)	270.4	(+52.5)	(+45.3)
pCCD-CISD+RDC	1.099	(-0.005)	(+0.001)	2360	(+19)	(+1)	234.4	(+16.5)	(+9.3)
fpLCCSD	1.102	(-0.002)	(+0.004)	2340	(-1)	(-19)			
fpCCSD	1.100	(-0.011)	(+0.002)	2365	(+24)	(+6)			
CCSD	1.093	(-0.011)	(-0.005)	2444	(+103)	(+85)			
MRCI ¹⁰⁵	1.104		(+0.006)	2341		(-18)	217.9		(-7.2)
exp ^{106,107}	1.098	(-0.006)		2359	(+18)		225.1	(+7.2)	

A. The Nitrogen Dimer

Figure 1 shows the PESs obtained from various pCCD-based methods and conventional single-reference CC models restricted to double and single and double excitations. We performed pCCD-CID and pCCD-CISD calculations with and without a renormalized Davidson correction (RDC). The corresponding results are indicated by including “+RDC” in the label. Furthermore, the superscripts ' indicates that the electron pair sector is included in CI calculations.

All investigated corrections generally predict a similar behavior around the equilibrium distances, while the shape of the PES features only small changes up to a bond distance of 1.6 Å. From this point onward, the PESs obtained from various pCCD-CI methods differ from those predicted by

fp(L)CC as well as conventional CC approaches. This observations is true for both variants, including only double (Figure 1-a) as well as single and double (Figure 1-b) excitations in the CI ansatz. Specifically, for interatomic distances of ≥ 2 Å, conventional methods as well as pCCD-based CC corrections diverge. On the other hand, the potential energy curves predicted by pCCD-CI are smooth and do not suffer from divergencies along the reaction coordinate. In the vicinity of dissociation (around 3 Å), the simple RD correction, however, breaks down and yields undershooting PESs. Nonetheless, a single-reference CI correction restricted to at most double excitations is able to provide a sound dissociation pathway for the N_2 molecule, while approaches based on CC corrections break down for stretched N–N bond lengths.

For a quantitative analysis, we determined the spectro-

scopic constants from the fitted PESs, which are summarized in Table I and compared to MRCI and experimental reference data, respectively. In general, all investigated CI and CC methods underestimate r_e and overestimate ω_e and D_e , respectively. Both the CID and CISD correction provide similar spectroscopic constants. Most importantly, including the electron pair sector in the CI ansatz considerably worsens vibrational frequencies and potential energy well depths, where the errors are approximately doubled and approach the CCD/CCSD level of accuracy. Including a Davidson correction on top of pCCD-CID or pCCD-CISD significantly lowers errors in spectroscopic constants by more than a factor of 2. In general, pCCD-CISD+RDC yields values for r_e and ω_e that lie between fpLCCSD and fpCCD accuracy, while fpLCCSD predicts spectroscopic constants closest to MRCI reference data. Conventional CC methods (CCD and CCSD) feature the largest deviations from MRCI and experimental reference data. We should note that a CI correction excluding the electron pair sector, but including a Davidson correction, yields results closest to experiment (with differences up to 0.001 Å, 1 cm⁻¹, or 9 kcal mol⁻¹ for r_e , ω_e , and D_e , respectively). A significant advantage of pCCD-CI methods over CC-type corrections is the ability to dissociate the N₂ molecule without encountering divergencies. Similar to r_e and ω_e , the most reliable results for D_e are obtained from pCCD-CISD+RDC (that is, excluding the electron pair sector). Although the fitted value of D_e deviates by about 4% from the experimental value, the absolute difference of 9 kcal mol⁻¹ is dissatisfying. Compared to MRCI reference data, this error further increases to 16 kcal mol⁻¹. In summary, pCCD-CI methods excluding the electron pair sector are more accurate than the corresponding CI flavours explicitly including electron pair excitations. Moreover, an RDC correction noticeably improves the performance of the proposed pCCD-CI models, significantly lowering the Δ_{MRCI} and Δ_{exp} errors. In general, pCCD-CI outperforms conventional CC methods of similar cost, provides spectroscopic constants between the fpLCC and fpCC level of accuracy, and can efficiently model the static/nondynamical and dynamical correlation along the reaction coordinate.

B. The Fluorine Dimer

In contrast to the N₂ molecule, we do not observe any significant differences in the shape of the PESs predicted by all investigated pCCD corrections for the F₂ dimer (see Figure 2). The similarities in the shape of the potential energy curves translate into similar values of spectroscopic constants, which are summarized in Table II. As expected, major differences (Δ_{MRCI}) are obtained if the electron pair sector is included in the CI ansatz. We should note that, in contrast to the N₂ dimer, Δ_{exp} for r_e and ω_e significantly decreases in CI' corrections, while errors in D_e considerably increase. Most importantly, the changes in spectroscopic constants are only minor if single excitations are included in the CI or CC correction. Moreover, the accuracy in spectroscopic constants is similar for pCCD-CI methods (without electron pair excitations) and fp(L)CC models. While pCCD-CI provides smaller errors in r_e and D_e ,

fp(L)CC yields values of ω_e that are closer to MRCI reference data. Specifically, both types of corrections overestimate r_e by around 0.02 (0.01) Å compared to experimental (MRCI) reference data, while the differences in D_e amount to approximately 10 kcal mol⁻¹. Furthermore, the proposed pCCD-CI methods increase the error in harmonic vibrational frequencies ω_e by about 10 cm⁻¹ with respect to fp(L)CC. Including a RD correction on top of the pCCD-CI models has only a minor effect on spectroscopic constants. While r_e remains unchanged, ω_e and D_e only marginally worsen by 3 cm⁻¹ and 0.4 kcal mol⁻¹. Finally, all pCCD corrections outperform the conventional CCD or CCSD models, which provide large errors in r_e (about 0.03 Å), ω_e (126 cm⁻¹), and D_e (about 36 kcal mol⁻¹).

To sum up, the quality and performance of the investigated CI corrections on top of a pCCD reference function is comparable to fp(L)CC methods featuring a similar excitation order. Nonetheless, for problems which feature a substantial amount of static electron correlation effects (like the dissociation process of N₂), the proposed pCCD-CI models seem more robust and less dependent on the quality of the pCCD reference. Thus, pCCD-CI might be less prone to unexpected failures encountered in CC corrections like divergencies.

V. ASSESSING THE ACCURACY OF CI CORRECTIONS IN ACTINIDE-CONTAINING COMPOUNDS

In the following, we extend our test set of light diatomic molecules with small di- and triatomic actinide compounds. Specifically, we investigate the simplest actinide compounds, ThO^{93,109–115} and ThS^{93,116} which are important systems in studies on the electron electric dipole moment (eEDM).^{93,117–120} Furthermore, we scrutinize the performance of the CI corrections for the the UO₂²⁺ isoelectronic series,^{91,92,121–135} containing UO₂²⁺, UN₂, PaO₂⁺ and ThO₂.^{91,130,135–142} Finally, we augment our numerical analysis to target also the lowest-lying excited states in the UO₂²⁺ cation.

A. Targeting the ground states of actinide compounds

The spectroscopic constants for the electronic ground states of the investigated actinide compounds are summarized in Table III and are obtained from the corresponding PESs, which are collected in the SI. For ThO, the inclusion of single excitations on top of doubles in the correction significantly improves the equilibrium distance r_e . This is a common feature for all investigated pCCD corrections, where fpLCCSD yields the most accurate values, which differ only about 0.003 Å from the CCSD(T) reference results. fpCCSD and pCCD-CISD+RDC (that is, including a RD correction) perform similarly, both underestimating r_e by about 0.009 Å. Similar observation can be made for the harmonic vibrational frequencies. Specifically, the LCCSD correction approaches spectroscopic accuracy (deviating by 2 cm⁻¹ from the reference),

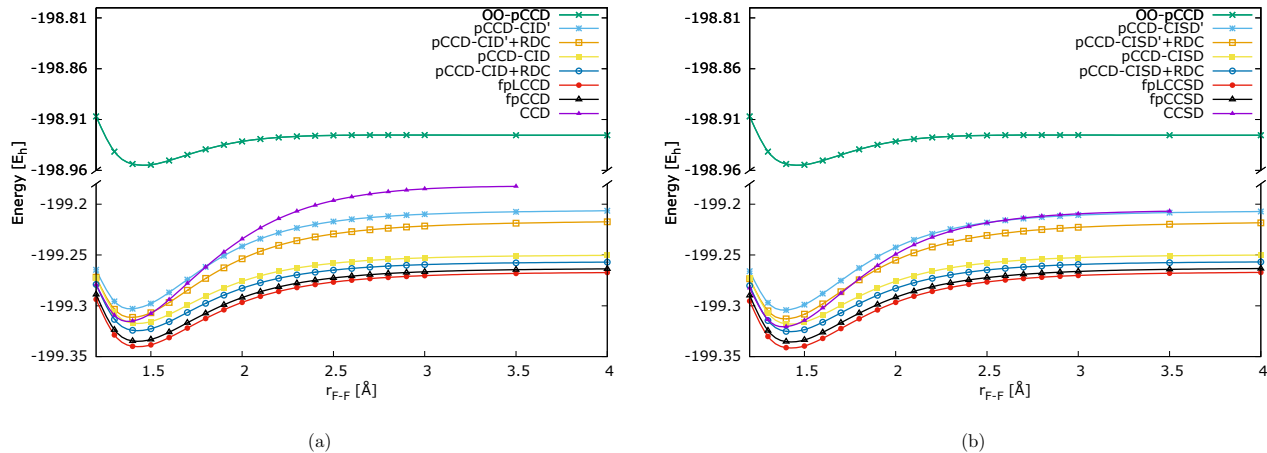


FIG. 2. Potential energy surfaces for the ground states of F_2 determined for various post-pCCD methods with (a) doubles excitation and (b) singles and doubles excitations. The superscript ' indicates that the CI operator also includes the electron pair sector. RDC: renormalized Davidson correction.

TABLE II. Spectroscopic parameters for the ground state of the F_2 molecule obtained from various post-pCCD methods and conventional CC models. r_e is the equilibrium bond length, ω_e the harmonic vibrational frequency, and D_e the dissociation energy, respectively. The differences with respect to experimental result Δ_{exp} or MRCI reference data Δ_{MRCI} are given in parentheses. The total electronic energies are summarized in the SI. RDC: renormalized Davidson correction.

Method	r_e [Å]	Δ_{MRCI}	Δ_{exp}	ω_e [cm^{-1}]	Δ_{MRCI}	Δ_{exp}	D_e [$\frac{\text{kcal}}{\text{mol}}$]	Δ_{MRCI}	Δ_{exp}
oo-pCCD	1.458	(+0.038)	(+0.046)	733	(-159)	(-184)	18.6	(-15.3)	(-18.7)
pCCD-CID'	1.397	(-0.023)	(-0.015)	975	(+83)	(+58)	60.5	(+26.6)	(+22.8)
pCCD-CID'+RDC	1.403	(-0.017)	(-0.009)	954	(+62)	(+37)	59.0	(+25.1)	(+21.3)
pCCD-CID	1.431	(+0.011)	(+0.019)	857	(-35)	(-60)	42.2	(+8.3)	(+4.5)
pCCD-CID+RDC	1.430	(+0.010)	(+0.018)	857	(-35)	(-60)	42.4	(+8.5)	(+4.7)
fpLCCSD	1.434	(+0.014)	(+0.022)	866	(-26)	(-51)	44.3	(+10.4)	(+6.6)
fpCCSD	1.433	(+0.013)	(+0.021)	863	(-29)	(-48)	43.3	(+9.4)	(+5.6)
CCD	1.383	(-0.037)	(-0.029)	1053	(+161)	(+136)	82.2	(+48.3)	(+44.5)
pCCD-CISD'	1.397	(-0.023)	(-0.015)	978	(+86)	(+71)	60.9	(+27.0)	(+23.2)
pCCD-CISD'+RDC	1.403	(-0.017)	(-0.009)	957	(+65)	(+40)	59.3	(+25.4)	(+21.6)
pCCD-CISD	1.429	(+0.009)	(+0.017)	864	(-28)	(-53)	42.7	(+8.8)	(+5.0)
pCCD-CISD+RDC	1.429	(+0.009)	(+0.017)	867	(-25)	(-50)	43.1	(+9.2)	(+5.4)
fpLCCSD	1.431	(+0.011)	(+0.019)	879	(-13)	(-38)	45.2	(+11.3)	(+7.5)
fpCCSD	1.431	(+0.011)	(+0.019)	873	(-19)	(-44)	44.2	(+10.3)	(+6.5)
CCSD	1.392	(-0.028)	(-0.020)	1018	(+126)	(+101)	70.1	(+36.2)	(+32.4)
MRCI ¹⁰⁵	1.420		(+0.008)	892		(-25)	33.9		(-3.8)
exp ^{106,108}	1.412	(-0.008)		917	(+25)		37.7	(+3.8)	

while fpCCSD and pCCD-CISD+RDC feature larger differences of about 36 and 33 cm^{-1} , respectively.

In case of the ThS molecule, all investigated pCCD corrections yield spectroscopic constants of similar accuracy. While all CI corrections and the conventional CCSD model underestimate r_e , the LCCSD correction overestimates equilibrium bond lengths. In absolute value, all corrections provide similar error measures amounting from 0.007 to 0.011 Å with respect to CCSD(T) reference values. The fitted values for ω_e are very consistent, where all corrections result in an error of approximately 20 cm^{-1} with respect to the CCSD(T) harmonic vibrational frequency. As observed above, adding a RD correction generally improves the performance of all pCCD-CI-type approaches. However, we should note that the pCCD approximation already delivers a well description of spectro-

scopic constants for both the ThO and ThS molecules. All applied corrections do not significantly improve the pCCD results.

Quantum chemistry studies on the UO_2^{2+} isoelectronic series are still an active field of research. These small triatomic molecules have a linear geometry beyond the ThO_2 species, which features a bent geometry and a peculiar electronic structure. In contrast to its linear analogues, the Thorium 5f orbitals of ThO_2 participate neither in bonding nor in electronic excitations. This is caused by differences in the relative energetic ordering of the 5f and 6d orbitals in the thorium and uranium atoms, respectively. By scrutinizing the spectroscopic constants summarized in Table III, we are able to assess whether the investigated post-pCCD methods can reliably model electron correlation effects in these compounds along

TABLE III. Spectroscopic parameters of the ground states of the investigated actinide-containing compounds obtained from various post-pCCD methods and conventional CC methods. r_e is the equilibrium bond length, ω_e the harmonic vibrational frequency, respectively. The differences with respect to CCSD(T) are given in parentheses. The total electronic energies, as also PES curves are summarized in the ESI†. RDC: renormalized Davidson correction.

Method	r_e [Å]	ω_e [cm ⁻¹]	r_e [Å]	ω_e [cm ⁻¹]	r_e [Å]	ω_e [cm ⁻¹]
	ThO		ThS		UO ₂ ⁺	
oo-pCCD	1.854 (-0.012)	894 (+56)	2.387 (+0.011)	484 (+12)	1.670 (-0.038)	1139 (+72)
pCCD-CID'	1.850 (-0.016)	898 (+60)	2.365 (-0.011)	494 (+22)	1.681 (-0.027)	1164 (+97)
pCCD-CID'+RDC	1.853 (-0.013)	890 (+52)	2.366 (-0.010)	492 (+20)	1.687 (-0.021)	1154 (+87)
pCCD-CID	1.854 (-0.012)	888 (+50)	2.366 (-0.010)	494 (+22)	1.687 (-0.021)	1129 (+62)
pCCD-CID+RDC	1.855 (-0.011)	886 (+48)	2.365 (-0.011)	493 (+21)	1.690 (-0.018)	1114 (+47)
fpLCCD	1.858 (-0.008)	876 (+38)	2.367 (-0.009)	488 (+16)	1.701 (-0.007)	1067 (±0)
fpCCD	1.856 (-0.010)	869 (+31)	2.365 (-0.011)	491 (+19)	1.698 (-0.010)	1087 (+20)
CCD	1.851 (-0.015)	895 (+57)	2.362 (-0.014)	492 (+20)	1.683 (-0.025)	1174 (+107)
pCCD-CISD'	1.852 (-0.014)	894 (+56)	2.368 (-0.008)	494 (+22)	1.683 (-0.025)	1158 (+91)
pCCD-CISD'+RDC	1.856 (-0.010)	889 (+51)	2.370 (-0.006)	487 (+15)	1.689 (-0.019)	1129 (+62)
pCCD-CISD	1.855 (-0.011)	889 (+51)	2.367 (-0.009)	492 (+20)	1.689 (-0.019)	1125 (+58)
pCCD-CISD+RDC	1.857 (-0.009)	871 (+33)	2.369 (-0.007)	487 (+15)	1.694 (-0.014)	1102 (+35)
fpLCCSD	1.863 (-0.003)	840 (+2)	2.384 (+0.008)	457 (-15)	1.717 (+0.009)	976 (-91)
fpCCSD	1.857 (-0.009)	874 (+36)	2.367 (-0.009)	489 (+17)	1.698 (-0.010)	1115 (+48)
CCSD	1.855 (-0.011)	885 (+47)	2.366 (-0.010)	487 (+15)	1.690 (-0.018)	1142 (+75)
CCSD(T)	1.866	838	2.376	472	1.708	1067
	ThO ₂		PaO ₂ ⁺		UN ₂	
oo-pCCD	1.917 (-0.012)	805 (-13)	1.763 (-0.021)	972 (±0)	1.711 (-0.030)	1176 (+74)
pCCD-CID'	1.913 (-0.016)	858 (+40)	1.763 (-0.021)	1024 (+52)	1.717 (-0.024)	1171 (+69)
pCCD-CID'+RDC	1.917 (-0.012)	841 (+23)	1.767 (-0.017)	1011 (+39)	1.722 (-0.019)	1164 (+62)
pCCD-CID	1.917 (-0.012)	852 (+34)	1.768 (-0.016)	1000 (+28)	1.720 (-0.021)	1124 (+22)
pCCD-CID+RDC	1.918 (-0.011)	850 (+32)	1.771 (-0.013)	987 (+15)	1.725 (-0.016)	1122 (+20)
fpLCCD	1.925 (-0.004)	829 (+11)	1.778 (-0.006)	995 (+23)	1.736 (-0.005)	1077 (-25)
fpCCD	1.924 (-0.005)	830 (+12)	1.776 (-0.008)	985 (+13)	1.731 (-0.011)	1102 (±0)
CCD	1.914 (-0.015)	850 (+32)	1.765 (-0.019)	1027 (+55)	1.722 (-0.019)	1184 (+82)
pCCD-CISD'	1.914 (-0.015)	851 (+33)	1.765 (-0.019)	1014 (+42)	1.719 (-0.022)	1162 (+40)
pCCD-CISD'+RDC	1.918 (-0.011)	842 (+24)	1.770 (-0.014)	1004 (+32)	1.725 (-0.016)	1152 (+50)
pCCD-CISD	1.918 (-0.011)	837 (+19)	1.770 (-0.014)	999 (+27)	1.722 (-0.019)	1118 (+16)
pCCD-CISD+RDC	1.920 (-0.009)	836 (+18)	1.774 (-0.010)	982 (+10)	1.727 (-0.014)	1106 (+4)
fpLCCSD	1.934 (+0.005)	773 (-45)	1.789 (+0.005)	895 (-77)	1.748 (+0.007)	960 (-142)
fpCCSD	1.923 (-0.006)	829 (+11)	1.776 (-0.008)	989 (+17)	1.733 (-0.008)	1113 (+11)
CCSD	1.918 (-0.011)	804 (-14)	1.770 (-0.014)	965 (-75)	1.727 (-0.014)	1158 (+56)
CCSD(T)	1.929	818	1.784	972	1.741	1102

the PESs. Starting from the uranyl cation, pCCD considerably underestimates the equilibrium distance r_e . All CI corrections significantly improve this value decreasing the errors by a factor of 2. Specifically, pCCD-CISD+RDC underestimate r_e by -0.014 Å. A better performance can be observed for fp(L)CC methods, which differ by only $0.007 - 0.009$ Å in absolute value. Predicting accurate ω_e is more challenging. In order to reduce the pCCD errors by a factor of 2, a CISD+RDC correction is required, while the remaining CI flavours feature large differences with respect to CCSD(T) reference values (more than 60 cm⁻¹). The performance of the fp(L)CC methods is more erratic. While fpLCCD predicts a ω_e that perfectly agrees with the CCSD(T) reference, inclusion of single excitations leads to large errors (up to 90 cm⁻¹). Moving to a fpCCSD formalism improves spectroscopic constants, where the errors in ω_e amount to 48 cm⁻¹. We should highlight that the conventional CCSD method provides larger errors in spectroscopic constants than the alternatives fp(L)CCSD or pCCD-CISD+RDC.

Analogous to the examples above, the CI corrections significantly improves pCCD results for the UN₂ molecule, where pCCD-CISD+RDC provides the smallest errors with respect

to CCSD(T) reference data. Furthermore, we observe the same tendency for all investigated corrections to underestimate the equilibrium bond length and to overestimate the harmonic vibrational frequency, except for fpLCCSD, which shows the opposite behaviour. Specifically, the (L)CCSD corrections provide more accurate equilibrium bond lengths, while the CISD flavours reduce the errors in ω_e to 4 cm⁻¹. Most importantly, fpCCSD and pCCD-CISD+RDC outperform the conventional CCSD approach and predict spectroscopic constants that deviate the least from CCSD(T) reference values.

For the protactinium dioxygen cation, we observe similar trends, where the CI/CC corrections are able to cure some of the deficiencies originated from the pCCD model. Specifically, the errors in r_e are reduced by a factor of 2 in CI-type corrections (pCCD-CISD+RDC features an error of 0.01 Å) and further lowered to 0.005 Å in the LCC corrections. However, all investigated pCCD corrections deteriorate harmonic vibrational frequencies, where pCCD already provides the proper shape of the PESs around the equilibrium distance. While pCCD-CISD+RDC yields the smallest errors of 10 cm⁻¹, fpLCCSD increases the discrepancy to 77

cm^{-1} . Nonetheless, both CID/CISD and (L)CCD/(L)CCSD corrections again outperform the conventional CCD/CCSD approaches, which feature one of the largest errors in spectroscopic constants.

A particular difficult case is the ThO_2 molecule, where the CI corrections do not significantly change or improve the spectroscopic constants derived from the pCCD PES. The best performance is obtained from the fp(L)CC methods, where the errors in r_e are reduced to 0.005 \AA , while the absolute errors in ω_e remain unchanged (except for fpLCCSD, which provides the largest errors). The most accurate CI flavor is again pCCD-CISD+RDC, which underestimates r_e by around 0.009 \AA , while ω_e deviates by 18 cm^{-1} . The performance of the CI corrections lies between fp(L)CC and conventional CC theory.

B. Dissecting the accuracy of pCCD corrections based on an error analysis.

To scrutinize the accuracy of the investigated corrections in predicting accurate values for r_e and ω_e , we perform a statistical analysis. Specifically, we evaluate the mean error (ME) of the fitted spectroscopic constants with respect to CCSD(T) reference data,

$$\text{ME} = \sum_i^N \Delta x_i / N, \quad (13)$$

where Δx_i is the difference in r_e or ω_e between a selected method and the reference $\Delta x_i = x_i^{\text{method}} - x_i^{\text{CCSD(T)}}$. The sum runs over the all investigated actinide-containing compounds ($N = 6$). Furthermore, we also determine the root-mean-square deviation (RMSD) in r_e and ω_e , according to

$$\text{RMSD} = \sqrt{\sum_i^N \Delta x_i^2 / N}. \quad (14)$$

The graphical representation of the ME and RMSD of r_e is shown in Figure 3 for CI and CC methods including (a) only double and (b) single and double excitations. On average, all investigated methods underestimate the equilibrium bond distance. The smallest deviations from CCSD(T) data are obtained from fpLCCD/fpLCCSD, followed by fpCCD/fpCCSD and then by pCCD-CID+RDC/pCCD-CISD+RDC. The largest discrepancies are deduced from the pCCD-CID'/pCCD-CISD' PESs. These large errors might be related to the double-counting problem of electron correlation effects associated with the electron pairs, which are included in both the pCCD reference function and the *a posteriori* CI correction. Excluding pair excitations in the CI operator significantly reduces errors. Furthermore, including single excitations in the pCCD correction only slightly affects equilibrium bond lengths, where the ME and RMSE are reduced by 0.002 \AA in CI corrections and by 0.001 \AA in the (L)CC flavors. However, the performance of fpLCC methods is more erratic; while fpCCD underestimates r_e , fpCCSD overestimates equilibrium distances. Finally, we

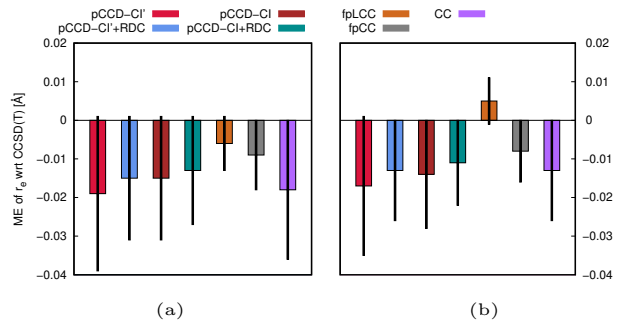


FIG. 3. Mean errors in r_e obtained for various post-pCCD and conventional CC methods restricted to (a) double excitations and (b) single and double excitations with respect to CCSD(T) reference data calculated from eq. 13 for all investigate actinide-containing compounds. The standard deviation (RMSE) is indicates as black lines. The corresponding numerical values are summarized in Table S19 in the SI. RDC: renormalized Davidson correction.

should note that all pCCD corrections (excluding the pair sector and including a RD correction) provide smaller ME and RMSE compared to the conventional CC methods featuring similar excitation operators.

Figure 4 highlights the ME and RMSD for ω_e for all CI and CC methods restricted to (a) double excitations and (b) single and double excitations. A similar behaviour in ME and RMSD can be observed as found for r_e . Considering only double excitations, fpLCCD yields the smallest ME of 10 cm^{-1} , followed by fpCCD with a ME up to 20 cm^{-1} , while pCCD-CID+RDC features an increased ME of about 30 cm^{-1} . All investigated approaches tend to overestimate the harmonic vibrational frequency. Note that the largest errors are obtained for the conventional CCD model. Including both single and double excitations significantly changes the distribution of ME and RMSE. The smallest ME is obtained for pCCD-CISD+RDC (19 cm^{-1}), followed by fpCCSD with a ME of about 23 cm^{-1} . Furthermore, the inclusion of single excitations in the correction significantly increases the accuracy of all CI-type corrections, while the ME of fpCC methods grows by about 70%. Similarly, the performance of fpLCC considerably deteriorates raising ME and RMSE by a factor of 6 and 4, respectively. To summarize, fpLCCSD provides the smallest errors in r_e , while pCCD-CISD+RDC properly describes the shape of the PESs yielding the most accurate harmonic vibrational frequencies.

C. Performance of pCCD-CI methods for excited states.

Finally, we will turn our discussion toward electronically excited states and scrutinize the performance of the investigated pCCD-CI methods to model the lowest-lying electronic states in the UO_2^{2+} molecule. Specifically, we target the following electronically excited states: $\sigma_u \rightarrow \delta_u$, $\sigma_u \rightarrow \phi_u$ and two $\pi_u \rightarrow \delta_u$ transitions. Our analysis is based on our previous study,⁶² where we focused on dissecting the accu-

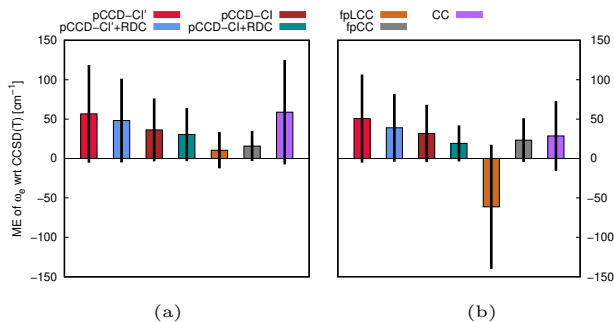


FIG. 4. Mean errors in ω_e obtained for various post-pCCD and conventional CC methods restricted to (a) double excitations and (b) single and double excitations with respect to CCSD(T) reference data calculated from eq. 13 for all investigate actinide-containing compounds. The standard deviation (RMSE) is indicates as black lines. The corresponding numerical values are summarized in Table S20 in the SI. RDC: renormalized Davidson correction.

racy of the LCC corrections in targeting electronically excited states in selected actinide compounds. As a reference method, we chose the completely renormalized equation of motion coupled cluster singles doubles and perturbative triples (CR-EOM-CCSD(T)) method.¹⁴⁴

Table IV contains the fitted spectroscopic constants for

TABLE IV. Spectroscopic constants of some low-lying singlet excited states of UO_2^{2+} obtained from various post-pCCD methods and conventional EOM-CC theory. r_e is the equilibrium bond length, ω_e the harmonic vibrational frequency, T_e the adiabatic excitation energy, and T_v the vertical excitation energy, respectively. T_v has been calculated with respect to the equilibrium bond distance r_e of the corresponding ground state obtained for each method. The differences with respect to CR-EOM-CCSD(T) are given in parentheses. The superscripts $'$ indicates that the pCCD-CISD method includes the electron pair sector in the excitation operator. EOM-fpLCCSD was originally introduces as EOM-pCCD-LCCSD.¹⁴³

Method	UO_2^{2+}			
	r_e [Å]	ω_e [cm^{-1}]	T_e [eV]	T_v [eV]
	$1^1\Phi_g(\sigma_u \rightarrow \phi_u)$			
pCCD-CISD'	1.773(+0.018)	888(-49)	14.50(+10.74)	14.92(+10.93)
pCCD-CISD	1.773(+0.018)	888(-49)	14.50(+10.74)	14.92(+10.93)
EOM-fpLCCSD	1.786(+0.031)	837(-100)	3.66(-0.10)	3.87(-0.12)
EOM-CCSD	1.762(+0.007)	924(-13)	3.57(-0.19)	3.86(-0.13)
CR-EOM-CCSD	1.755	937	3.76	3.99
	$1^1\Delta_g(\sigma_u \rightarrow \delta_u)$			
pCCD-CISD'	1.791(+0.039)	764(-169)	14.72(+10.56)	15.17(+10.80)
pCCD-CISD	1.791(+0.039)	764(-169)	14.72(+10.56)	15.17(+10.80)
EOM-fpLCCSD	1.781(+0.029)	840(-93)	4.07(-0.09)	4.25(-0.12)
EOM-CCSD	1.760(+0.008)	910(-23)	3.96(-0.20)	4.22(-0.15)
CR-EOM-CCSD	1.752	933	4.16	4.37
	$2^1\Phi_g(\pi_u \rightarrow \delta_u)$			
pCCD-CISD'	1.803(+0.013)	928(+22)	14.75(+9.85)	15.34(+9.89)
pCCD-CISD	1.801(+0.012)	975(+69)	14.74(+9.84)	15.34(+9.89)
EOM-fpLCCSD	1.804(+0.014)	941(+35)	4.87(-0.03)	5.29(-0.16)
EOM-CCSD	1.797(+0.007)	902(-4)	4.46(-0.44)	5.08(-0.37)
CR-EOM-CCSD(T)	1.790	906	4.90	5.45
	$1^1\Pi_g(\pi_u \rightarrow \delta_u)$			
pCCD-CISD'	1.784(-0.006)	1023(+118)	14.83(+9.84)	15.53(+10.00)
pCCD-CISD	1.785(-0.005)	1042(+137)	14.82(+9.83)	15.52(+9.99)
EOM-fpLCCSD	1.804(+0.014)	965(+60)	4.98(-0.01)	5.38(-0.15)
EOM-CCSD	1.796(-0.006)	904(-1)	4.55(-0.44)	5.16(-0.37)
CR-EOM-CCSD(T)	1.790	905	4.99	5.53

the four lowest-lying targeted excited states. pCCD-CISD with and without electron pair excitations yield equivalent results (for r_e and excitation energies) due to the purely singly-excited character of the targeted states. However, the excitation energies predicted by the CI corrections strongly deviate from all EOM-CC results. While the ground state energies are corrected towards lower energies (by accounting for the missing dynamical correlation energy), all electronically excited states miss this shift in energy. Although pCCD-CISD provides reasonable excitation energies with respect to the pCCD reference energy, it misses a large fraction of the dynamical correlation energy of the excited states. The adiabatic and vertical excitation energies collected in Table IV demonstrate that this shift in energy between pCCD-CISD and the CCSD/CR-EOM-CCSD(T) reference amounts to over 10 eV. This disproportion in excitation energies is significant, especially compared to EOM-fpLCCSD, which differs only around from 0.1 to 0.5 eV from reference values. Although these quantitative deficiencies of pCCD-CISD methods in capturing electron correlation effects in excited states forbid us to precisely target excitation energies, the CI corrections predict equilibrium bond lengths with reasonable accuracy providing smaller differences from CR-EOM-CCSD(T) reference data than EOM-fpLCCSD. The prediction of harmonic vibrational frequencies is, however, more erratic, where errors lie between 12 and 140 cm^{-1} . Specifically, for the lowest excited state $1^1\Phi_g$, pCCD-CISD predicts spectroscopic constants that are closer to reference values than the corresponding EOM-fpLCCSD results. Thus, pCCD-CISD generally fails in describing electronically excited states and provides spectroscopic constants of irregular accuracy. Similar disadvantages of CI corrections in predicting excitation energies were noticed in previous numerical studies.⁷¹

VI. CONCLUSIONS

In this work, we developed various CI corrections with a pCCD references function that are restricted to at most double (hole-particle) excitations. Furthermore, we tested CI models, where the linear CI operator excludes and includes electron pair excitations, where the former case might be important to properly describe doubly-excited states. The accuracy of the proposed pCCD-CI approaches was assessed for the ground states of light diatomic molecules, namely F_2 and N_2 , as well as for selected di- and tri-atomic f0 actinide species, such as the ThO , ThS , UO_2^{2+} , NUN , PaO_2^+ , and ThO_2 molecules. We also scrutinized the performance of the CI corrections on the lowest-lying electronically excited states in the UO_2^{2+} cation. The CI corrections were compared to fp(L)CC methods as well as to conventional CC variants. Finally, we introduced a simple renormalized Davidson correction to minimize size-consistency errors in the ground state electronic structures.

Our study demonstrates that the proposed pCCD-CI methods provide a reliable and promising alternative to conventional CC methods as well as to the other unconventional approaches such as the fp(L)CC model. A major advantage of the CI-type corrections is their ability to dissociate the N_2

molecule, where the contributions to electron correlation effects change along the reaction coordinate. The accuracy of the pCCD-CI models can be improved by including an (approximate) renormalized Davidson correction, where the errors in spectroscopic constants are reduced by a factor of 2. In general, pCCD-CISD+RDC allows us to obtain smooth PESs and predicts spectroscopic constants that agree well with experimental or MRCI reference data. Specifically, pCCD-CISD+RDC outperforms conventional CCSD, while the spectroscopic constants lie between fpLCCSD and fpCCSD accuracy. The good performance of pCCD-CISD+RDC is also observed for heavy-element-containing systems, where it features the smallest ME and RMSE in ω_e , while the corresponding error measures for r_e are slightly smaller than the CCSD values. The inclusion of electron-pair excitations in the CI operator, however, deteriorates the performance of the various CI corrections, which might originate from a double-counting problem of correlation effects associated with electron pair states as they are included in both the pCCD reference function and the *a posteriori* CI correction.

Finally, the pCCD-CISD model fails for electronically excited states, where large errors in excitation energies are observed. Although pCCD-CISD provides more accurate values for r_e in electronic excited states than the EOM-fpLCCSD model, the prediction of ω_e and (adiabatic and vertical) excitation energies is rather erratic. To sum up, a CI correction (including a Davidson correction) on top of pCCD is a promising alternative to conventional (like CCSD) or unconventional (like fp(L)CC) CC methods to model electronic ground states. However, in order to reach chemical or spectroscopic accuracy, further improvements are required, like approximate protocols to account for higher-order excitations. Furthermore, in this work, the CI operators are restricted to singlet excitations, while the projection manifold has been defined to allow for an algebraic spin-summation. By eliminating this constraint, the CI corrections would allow us to target different spin sectors. If we restrict the excitation operators to be of SD-type, both singlet and triplet states will be accessible in the CI corrections. The corresponding diagonalization problem has to be performed in the Slater determinant basis containing all singly- and doubly-excited determinants with respect to $|\Phi_0\rangle$ instead of the spin-summed states defined in eqs. (10) and (11). This formulation, however, increases the number of degrees of freedom of the diagonalization problem.

VII. DATA AVAILABILITY STATEMENT

The data that supports the findings of this study are available within the article and its supplementary material.

ACKNOWLEDGMENTS

A.N. and K.B. acknowledge financial support from a SONATA BIS grant of the National Science Centre, Poland (no. 2015/18/E/ST4/00584). A.N. also received financial support from a PRELUDIUM 17 grant of the National Science

Centre, Poland (no. 2019/33/N/ST4/01880).

- ¹B. Jeziorski, "Multireference coupled-cluster Ansatz," *Mol. Phys.* **108**, 3043–3054 (2010).
- ²D. I. Lyakh, M. Musiał, V. F. Lotrich, and J. Bartlett, "Multireference Nature of Chemistry: The Coupled-Cluster View," *Chem. Rev.* **112**, 182–243 (2012).
- ³V. V. Ivanov, D. I. Lyakh, and L. Adamowicz, "Multireference state-specific coupled-cluster methods. State-of-the-art and perspectives," *Phys. Chem. Chem. Phys.* **11**, 2355–2370 (2009).
- ⁴S. R. White, "Density matrix formulation for quantum renormalization groups," *Phys. Rev. Lett.* **69**, 2863–2866 (1992).
- ⁵S. R. White, "Density-matrix algorithms for quantum renormalization groups," *Phys. Rev. B* **48**, 10345–10356 (1993).
- ⁶S. R. White and R. L. Martin, "Ab initio quantum chemistry using the density matrix renormalization group," *J. Chem. Phys.* **110**, 4127–4130 (1999).
- ⁷O. Legeza, R. M. Noack, J. Sólyom, and L. Tincani, "Applications of Quantum Information in the Density-Matrix Renormalization Group," in *Computational Many-Particle Physics*, Lect. Notes Phys., Vol. 739, edited by H. Fehske, R. Schneider, and A. Weiße (Springer, Berlin/Heidelberg, 2008) pp. 653–664.
- ⁸K. H. Marti and M. Reiher, "The Density Matrix Renormalization Group Algorithm in Quantum Chemistry," *Z. Phys. Chem.* **224**, 583–599 (2010).
- ⁹G. K.-L. Chan and S. Sharma, "The Density Matrix Renormalization Group in Quantum Chemistry," *Annu. Rev. Phys. Chem.* **62**, 465–481 (2011).
- ¹⁰S. Szalay, M. Pfeffer, V. Murg, G. Barcza, F. Verstraete, R. Schneider, and Ö. Legeza, "Tensor product methods and entanglement optimization for ab initio quantum chemistry," *Int. J. Quantum Chem.* **115**, 1342–1391 (2015).
- ¹¹J. Hachmann, W. Cardoen, and G. K.-L. Chan, "Multireference correlation in long molecules with the quadratic scaling density matrix renormalization group," *J. Chem. Phys.* **125**, 144101 (2006).
- ¹²Y. Kurashige and T. Yanai, "High-performance ab initio density matrix renormalization group method: Applicability to large-scale multireference problems for metal compounds," *J. Chem. Phys.* **130**, 234114 (2009).
- ¹³T. Yanai, Y. Kurashige, W. Mizukami, J. Chalupsky, T. N. Lan, and M. Saitow, "Density matrix renormalization group for ab initio Calculations and associated dynamic correlation methods: A review of theory and applications," *Int. J. Quantum Chem.* **115**, 283–299 (2015).
- ¹⁴A. Baiardi and M. Reiher, "The density matrix renormalization group in chemistry and molecular physics: Recent developments and new challenges," *J. Chem. Phys.* **152**, 040903 (2020).
- ¹⁵K. Gunst, F. Verstraete, S. Wouters, O. Legeza, and D. Van Neck, "T3NS: Three-Legged Tree Tensor Network States," *J. Chem. Theory Comput.* **14**, 2026–2033 (2018).
- ¹⁶Y. Ma, S. Knecht, S. Keller, and M. Reiher, "Second-Order Self-Consistent-Field Density-Matrix Renormalization Group," *J. Chem. Theory Comput.* **13**, 2533–2549 (2017).
- ¹⁷S. Zhang, "Auxiliary-Field Quantum Monte Carlo for Correlated Electron Systems. Emergent Phenomena in Correlated Matter: Autumn School Organized by the Forschungszentrum Jülich and the German Research School for Simulation Sciences at Forschungszentrum Jülich 23–27 September 2013," *Lecture Notes of the Autumn School Correlated Electrons* **3**, 2013 (2013).
- ¹⁸S. Hochkeppel, T. C. Lang, C. Brünger, F. F. Assaad, and W. Hanke, "High Performance Computing in Science and Engineering, Garching/Munich 2007: Transactions of the Third Joint HLRB and KONWIHR Status and Result Workshop, Dec. 3–4, 2007, Leibniz Supercomputing Centre, Garching/Munich, Germany," (Springer Berlin Heidelberg, Berlin, Heidelberg, 2009) Chap. Quantum Monte Carlo Studies of Strongly Correlated Electron Systems, pp. 669–686.
- ¹⁹P. Tecmer and K. Boguslawski, "Geminal-based electronic structure methods in quantum chemistry. Toward a geminal model chemistry," *Phys. Chem. Chem. Phys.*, – (2022).
- ²⁰A. J. Coleman, "Structure of Fermion Density Matrices. II. Antisymmetrized Geminal Powers," *J. Math. Phys.* **6**, 1425–1431 (1965).
- ²¹S. Bratoz and P. Durand, "Transposition of the Theories Describing Superconducting Systems to Molecular Systems. Method of Biorbitals," *J. Chem. Phys.* **43**, 2670–2679 (1965).

- ²²D. M. Silver, "Natural Orbital Expansion of Interacting Geminals," *J. Chem. Phys.* **50**, 5108–5116 (1969).
- ²³D. M. Silver, "Bilinear Orbital Expansion of Geminal-Product Correlated Wavefunctions," *J. Chem. Phys.* **52**, 299–303 (1970).
- ²⁴G. Nary-Szabo, "All-pair wavefunction for many-electron states with the highest multiplicity," *J. Chem. Phys.* **58**, 1775–1776 (1973).
- ²⁵G. Nary-Szabo, "All-pair wave function and reduced variational equation for electronic systems," *Int. J. Quantum Chem.* **9**, 9–21 (1975).
- ²⁶A. C. Hurley, J. Lennard-Jones, and J. A. Pople, "The molecular orbital theory of chemical valency XVI. A theory of paired-electrons in polyatomic molecules," *Proc. R. Soc. Lond. A* **220**, 446–455 (1953).
- ²⁷J. M. Parks and R. G. Parr, "Theory of Separated Electron Pairs," *J. Chem. Phys.* **28**, 335–345 (1958).
- ²⁸E. Kapuy, "Applicability of almost strongly orthogonal geminals in many-electron wavefunctions," *J. Chem. Phys.* **44**, 956–962 (1966).
- ²⁹W. Kutzelnigg, "Direct Determination of Natural Orbitals and Natural Expansion Coefficients of Many-Electron Wavefunctions. I. Natural Orbitals in the Geminal Product Approximation," *J. Chem. Phys.* **40**, 3640–2647 (1964).
- ³⁰P. R. Surjan, "Interaction of chemical bonds: Strictly localized wave functions in orthogonal basis," *Phys. Rev. A* **30**, 43–50 (1984).
- ³¹P. R. Surjan, "Interaction Of Chemical Bonds. II. Ab Initio Theory For Overlap, Delocalization, And Dispersion Interactions," *Phys. Rev. A* **32**, 748–755 (1985).
- ³²P. R. Surjan, "The interaction of chemical bonds. III. Perturbed strictly localized geminals in LMO basis," *Int. J. Quantum Chem.* **52**, 563–574 (1994).
- ³³P. R. Surjan, "The interaction of chemical bonds. IV. Interbond charge transfer by a coupled-cluster-type formalism," *Int. J. Quantum Chem.* **55**, 109–116 (1995).
- ³⁴P. R. Surjan, "An Introduction to the Theory of Geminals," in *Correlation and Localization* (Springer, 1999) pp. 63–88.
- ³⁵E. Rosta and P. R. Surjan, "Interaction of chemical bonds. V. Perturbative corrections to geminal-type wave functions," *Int. J. Quantum Chem.* **80**, 96–104 (2000).
- ³⁶P. R. Surjan, . Szabados, P. Jeszenszki, and T. Zoboki, "Strongly orthogonal geminals: size-extensive and variational reference states," *J. Math. Chem.* **50**, 534–551 (2012).
- ³⁷V. A. Rassolov, "A geminal model chemistry," *J. Chem. Phys.* **117**, 5978–5987 (2002).
- ³⁸V. A. Rassolov, F. Xu, and S. Garashchuk, "Geminal model chemistry ii. perturbative corrections," *J. Chem. Phys.* **120**, 10385–10394 (2004).
- ³⁹B. A. Cagg and V. A. Rassolov, " SS_pG : A strongly orthogonal geminal method with relaxed strong orthogonality," *J. Chem. Phys.* **141**, 164112 (2014).
- ⁴⁰P. A. Johnson, P. W. Ayers, P. A. Limacher, S. De Baerdemacker, D. Van Neck, and P. Bultinck, "A Size-Consistent Approach to Strongly Correlated Systems Using a Generalized Antisymmetrized Product of Nonorthogonal Geminals," *Comput. Chem. Theory* **1003**, 101–113 (2013).
- ⁴¹P. A. Johnson, P. A. Limacher, T. D. Kim, M. Richer, R. A. Miranda-Quintana, F. Heidar-Zadeh, P. W. Ayers, P. Bultinck, S. De Baerdemacker, and D. Van Neck, "Strategies for extending geminal-based wavefunctions: Open shells and beyond," *Comput. Theor. Chem.* **1116**, 207–219 (2017).
- ⁴²P. A. Johnson, C.-. Fecteau, F. Berthiaume, S. Cloutier, L. Carrier, M. Gratton, P. Bultinck, S. De Baerdemacker, D. Van Neck, P. Limacher, *et al.*, "Richardson–gaudin mean-field for strong correlation in quantum chemistry," *J. Chem. Phys.* **153**, 104110 (2020).
- ⁴³C.-. Fecteau, F. Berthiaume, M. Khalfoun, and P. A. Johnson, "Richardson-gaudin geminal wavefunctions in a slater determinant basis," *J. Mat. Chem.* **59**, 289–301 (2021).
- ⁴⁴C.-. Fecteau, S. Cloutier, J.-D. Moisset, J. Boulay, P. Bultinck, A. Faribault, and P. A. Johnson, "Near-exact treatment of seniority-zero ground and excited states with a richardson–gaudin mean-field," *J. Chem. Phys.* **156**, 194103 (2022).
- ⁴⁵P. A. Limacher, P. W. Ayers, P. A. Johnson, S. De Baerdemacker, D. Van Neck, and P. Bultinck, "A New Mean-Field Method Suitable for Strongly Correlated Electrons: Computationally Facile Antisymmetric Products of Nonorthogonal Geminals," *J. Chem. Theory Comput.* **9**, 1394–1401 (2013).
- ⁴⁶K. Boguslawski, P. Tecmer, P. W. Ayers, P. Bultinck, S. De Baerdemacker, and D. Van Neck, "Efficient description of strongly correlated electrons with mean-field cost," *Phys. Rev. B* **89**, 201106(R) (2014).
- ⁴⁷T. Stein, T. M. Henderson, and G. E. Scuseria, "Seniority zero pair coupled cluster doubles theory," *J. Chem. Phys.* **140**, 214113 (2014).
- ⁴⁸K. Boguslawski, P. Tecmer, P. A. Limacher, P. A. Johnson, P. W. Ayers, P. Bultinck, S. De Baerdemacker, and D. Van Neck, "Projected seniority-two orbital optimization of the antisymmetric product of one-reference orbital geminal," *J. Chem. Phys.* **140**, 214114 (2014).
- ⁴⁹K. Boguslawski, P. Tecmer, P. W. Ayers, P. Bultinck, S. De Baerdemacker, and D. Van Neck, "Non-Variational Orbital Optimization Techniques for the AP1roG Wave Function," *J. Chem. Theory Comput.* **10**, 4873–4882 (2014).
- ⁵⁰K. Boguslawski, P. Tecmer, and . Legeza, "Analysis of two-orbital correlations in wavefunctions restricted to electron-pair states," *Phys. Rev. B* **94**, 155126 (2016).
- ⁵¹P. Tecmer, K. Boguslawski, P. A. Limacher, P. A. Johnson, M. Chan, T. Verstraelen, and P. W. Ayers, "Assessing the Accuracy of New Geminal-Based Approaches," *J. Phys. Chem. A* **118**, 9058–9068 (2014).
- ⁵²T. M. Henderson, I. W. Bulik, T. Stein, and G. E. Scuseria, "Seniority-based coupled cluster theory," *J. Chem. Phys.* **141**, 244104 (2014).
- ⁵³K. Boguslawski and P. Tecmer, "Orbital entanglement in quantum chemistry," *Int. J. Quantum Chem.* **115**, 1289–1295 (2015).
- ⁵⁴K. Boguslawski and P. Tecmer, "Erratum: Orbital entanglement in quantum chemistry," *Int. J. Quantum Chem.* **117**, e25455 (2017).
- ⁵⁵P. Tecmer, K. Boguslawski, and P. W. Ayers, "Singlet ground state actinide chemistry with geminals," *Phys. Chem. Chem. Phys.* **17**, 14427–14436 (2015).
- ⁵⁶A. J. Garza, A. G. S. Alencar, and G. E. Scuseria, "Actinide chemistry using singlet-paired coupled cluster and its combinations with density functionals," *J. Chem. Phys.* **143**, 244106 (2015).
- ⁵⁷K. Boguslawski and P. W. Ayers, "Linearized Coupled Cluster Correction on the Antisymmetric Product of 1-Reference Orbital Geminals," *J. Chem. Theory Comput.* **11**, 5252–5261 (2015).
- ⁵⁸K. Boguslawski and P. Tecmer, "Benchmark of Dynamic Electron Correlation Models for Seniority-Zero Wave Functions and Their Application to Thermochemistry," *J. Chem. Theory Comput.* **13**, 5966–5983 (2017).
- ⁵⁹F. Brzek, K. Boguslawski, P. Tecmer, and P. S. uchowski, "Benchmarking the Accuracy of Seniority-Zero Wave Function Methods for Noncovalent Interactions," *J. Chem. Theory Comput.* **15**, 4021–4035 (2019).
- ⁶⁰F. Kossoski, A. Marie, A. Scemama, M. Caffarel, and P.-F. Loos, "Excited states from state-specific orbital-optimized pair coupled cluster," *J. Chem. Theory Comput.* **17**, 4756–4768 (2021).
- ⁶¹P. Tecmer, K. Boguslawski, M. Borkowski, P. S. uchowski, and D. Kedziera, "Modeling the electronic structures of the ground and excited states of the ytterbium atom and the ytterbium dimer: A modern quantum chemistry perspective," *Int. J. Quantum Chem.* **119**, e25983 (2019).
- ⁶²A. Nowak, P. Tecmer, and K. Boguslawski, "Assessing the accuracy of simplified coupled cluster methods for electronic excited states in f0 actinide compounds," *Phys. Chem. Chem. Phys.* **21**, 19039–19053 (2019).
- ⁶³A. Leszczyk, P. Tecmer, and K. Boguslawski, in *Transition Metals in Coordination Environments, Challenges and Advances in Computational Chemistry and Physics*, Vol. 29 (Springer, Cham (Switzerland), 2019) Chap. New Strategies in Modeling Electronic Structures and Properties with Applications to Actinides, pp. 121–160.
- ⁶⁴E. Rosta and P. R. Surjan, "Two-Body Zeroth Order Hamiltonians In Multireference Perturbation Theory: The APSG Reference State," *J. Chem. Phys.* **116**, 878–889 (2002).
- ⁶⁵O. Christiansen, H. Koch, and P. Jorgensen, "Perturbative triple excitation corrections to coupled cluster singles and doubles excitation energies," *J. Chem. Phys.* **105**, 1451–1459 (1996).
- ⁶⁶P. Limacher, P. Ayers, P. Johnson, S. De Baerdemacker, D. Van Neck, and P. Bultinck, "Simple and inexpensive perturbative correction schemes for antisymmetric products of nonorthogonal geminals," *Phys. Chem. Chem. Phys.* **16**, 5061–5065 (2014).
- ⁶⁷T. Zoboki, A. Szabados, and P. R. Surjan, "Linearized Coupled Cluster Corrections to Antisymmetrized Product of Strongly Orthogonal Geminals : Role of Dispersive Interactions," *J. Chem. Theory Comput.* **9**, 2602–2608 (2013).

- ⁶⁸A. Leszczyk, M. Máté, Ö. Legeza, and K. Boguslawski, "Assessing the Accuracy of Tailored Coupled Cluster Methods Corrected by Electronic Wave Functions of Polynomial Cost," *J. Chem. Theory Comput.* **18**, 96–117 (2022).
- ⁶⁹A. J. Garza, I. W. Bulik, T. M. Henderson, and G. E. Scuseria, "Range separated hybrids of pair coupled cluster doubles and density functionals," *Phys. Chem. Chem. Phys.* **17**, 22412–22422 (2015).
- ⁷⁰A. J. Garza, I. W. Bulik, T. M. Henderson, and G. E. Scuseria, "Synergy between pair coupled cluster doubles and pair density functional theory," *J. Chem. Phys.* **142**, 044109 (2015).
- ⁷¹M. Kállay and P. Surján, "Improving CISD calculations by geminal-type reference states," *Chem. Phys. Lett.* **312**, 221–228 (1999).
- ⁷²I. Røeggen, "Electron correlation described by extended geminal models: The EXGEM4 and EXGEM5 models," *Int. J. Quantum Chem.* **31**, 951–974 (1987).
- ⁷³E. A. Carter and W. A. Goddard III, "Correlation-consistent configuration interaction: Accurate bond dissociation energies from simple wave functions," *J. Chem. Phys.* **88**, 3132–3140 (1988).
- ⁷⁴F. Faglioni and W. A. Goddard III, "GVB-RP: A reliable MCSCF wave function for large systems," *Int. J. Quantum Chem.* **73**, 1–22 (1999).
- ⁷⁵I. Røeggen, "Extended geminal models," in *Correlation and Localization* (Springer, 1999) pp. 89–103.
- ⁷⁶T. M. Henderson and G. E. Scuseria, "Geminal-based configuration interaction," *J. Chem. Phys.* **151**, 051101 (2019).
- ⁷⁷D. J. Rowe, "Equations-of-motion method and extended shell model," *Rev. Mod. Phys.* **40**, 153–166 (1968).
- ⁷⁸J. Geersten, M. Rittby, and R. J. Bartlett, "The equation-of-motion coupled cluster method: excitation energies of Be and CO," *Chem. Phys. Lett.* **164**, 57–62 (1989).
- ⁷⁹K. Kowalski, J. R. Hammond, W. A. de Jong, P.-D. Fan, M. Valiev, D. Wang, and N. Govind, "Coupled-cluster calculations for large molecular and extended systems," in *Computational Methods for Large Systems* (Wiley-Blackwell, 2011) Chap. 5, pp. 167–200.
- ⁸⁰A. I. Krylov, "Equation-of-motion coupled-cluster methods for open-shell and electronically excited species: The hitchhiker's guide to fock space," *Ann. Rev. Phys. Chem.* **59**, 433–462 (2008).
- ⁸¹Helgaker, T., Jørgensen, P., Olsen, J., *Molecular Electronic-Structure Theory* (Wiley, New York, 2000).
- ⁸²P. G. Szalay, "Configuration interaction: Corrections for size-consistency," in *Encyclopedia of Computational Chemistry* (John Wiley & Sons, Ltd, 2005).
- ⁸³P. G. Szalay, T. Müller, G. Gidofalvi, H. Lischka, and R. Shepard, "Multiconfiguration self-consistent field and multireference configuration interaction methods and applications," *Chem. Rev.* **112**, 108–181 (2012).
- ⁸⁴W. L. Luken, "Unlinked cluster corrections for configuration interaction calculations," *Chem. Phys. Lett.* **58**, 421–424 (1978).
- ⁸⁵T. Dunning Jr., "Gaussian basis sets for use in correlated molecular calculations. I. The atoms boron through neon and hydrogen," *J. Chem. Phys.* **90**, 1007–1023 (1989).
- ⁸⁶K. A. Peterson, "Correlation consistent basis sets for actinides. I. The Th and U atoms," *J. Chem. Phys.* **142**, 074105 (2015).
- ⁸⁷M. Reiher and A. Wolf, "Exact Decoupling of the Dirac Hamiltonian. I. General Theory," *J. Chem. Phys.* **121**, 2037–2047 (2004).
- ⁸⁸M. Reiher and A. Wolf, "Exact decoupling of the Dirac Hamiltonian. II. The generalized Douglas–Kroll–Hess transformation up to arbitrary order," *J. Chem. Phys.* **121**, 10945–10956 (2004).
- ⁸⁹M. Reiher and A. Wolf, *Relativistic Quantum Chemistry. The Fundamental Theory of Molecular Science* (Wiley, 2009).
- ⁹⁰Tecmer, P., Boguslawski, K., Kędziera, D., "Relativistic Methods in Computational Quantum Chemistry," in *Handbook of Computational Chemistry*, Vol. 2, edited by J. Leszczyński (Springer Netherlands, Dordrecht, 2017) pp. 885–926.
- ⁹¹F. Réal, A. S. P. Gomes, L. Visscher, V. Vallet, and E. Eliav, "Benchmarking Electronic Structure Calculations on the Bare UO_2^{2+} Ion: How Different are Single and Multireference Electron Correlation Methods?" *J. Phys. Chem. A* **113**, 12504–12511 (2009).
- ⁹²P. Tecmer, A. S. P. Gomes, S. Knecht, and L. Visscher, "Communication: Relativistic Fock-Space Coupled Cluster Study of Small Building Blocks of Larger Uranium Complexes," *J. Chem. Phys.* **141**, 041107 (2014).
- ⁹³P. Tecmer and C. E. González-Espinoza, "Electron correlation effects of the ThO and ThS molecules in the spinor basis. A relativistic coupled cluster study of ground and excited states properties," *Phys. Chem. Chem. Phys.* **20**, 23424–23432 (2018).
- ⁹⁴K. Boguslawski, A. Leszczyk, A. Nowak, F. Brzęk, P. S. Żuchowski, D. Kędziera, P. Tecmer, and P. Tecmer, "Pythonic Black-box Electronic Structure Tool (PyBEST). An open-source Python platform for electronic structure calculations at the interface between chemistry and physics," *Comput. Phys. Commun.* **264**, 107933 (2021).
- ⁹⁵F. Brzęk, A. Leszczyk, A. Nowak, E. Sujkowski, K. Boguslawski, D. Kędziera, P. Tecmer, P. S. Żuchowski, R. Chakraborty, M. Kriebel, and L. Szczuczko, "Pythonic Black-box Electronic Structure Tool (PyBEST v1.2.0)," (2022), Zenodo, 10.5281/zenodo.6787323.
- ⁹⁶(2022), see <http://pybest.fizyka.umk.pl> for more information about PyBEST (accessed September 22, 2022).
- ⁹⁷H.-J. Werner, P. J. Knowles, R. Lindh, F. R. Manby, P. C. M. Schütz, T. Korona, A. Mitrushenkov, G. Rauhut, T. B. Adler, R. D. Amos, A. Bernhardsson, A. Berning, D. L. Cooper, M. J. O. Deegan, A. J. Dobbyn, F. Eckert, E. Goll, C. Hampel, G. Hetzer, T. Hrenar, G. Knizia, C. Köppl, Y. Liu, A. W. Lloyd, R. A. Mata, A. J. May, S. J. McNicholas, W. Meyer, M. E. Mura, A. Nicklass, P. Palmieri, K. Pflüger, R. Pitzer, M. Reiher, U. Schumann, H. Stoll, A. J. Stone, R. Tarroni, T. Thorsteinsson, M. Wang, and A. Wolf, "Molpro, version 2009.1, a package of *ab initio* programs," (2009), see <http://www.molpro.net>.
- ⁹⁸M. Abramowitz and I. A. Stegun, *Handbook Of Mathematical Functions With Formulas, Graphs, And Mathematical Tables* (Dover, New York, 1970).
- ⁹⁹J. E. Sansonetti and W. C. Martin, "Handbook of basic atomic spectroscopic data," *J. Phys. Chem. Ref. Data* **34**, 1559–2259 (2005).
- ¹⁰⁰G. K.-L. Chan, M. Kállay, and J. Gauss, "State-of-the-art density matrix renormalization group and coupled cluster theory studies of the nitrogen binding curve," *J. Chem. Phys.* **121**, 6110–6116 (2004).
- ¹⁰¹K. Boguslawski, P. Tecmer, O. Legeza, and M. Reiher, "Entanglement Measures for Single- and Multireference Correlation Effects," *J. Phys. Chem. Lett.* **3**, 3129–3135 (2012).
- ¹⁰²K. Boguslawski, F. Réal, P. Tecmer, C. Duperrouzel, A. S. P. Gomes, Ö. Legeza, P. W. Ayers, and V. Vallet, "On the multi-reference nature of plutonium oxides: PuO_2^{2+} , PuO_2 , PuO_3 and $\text{PuO}_2(\text{OH})_2$," *Phys. Chem. Chem. Phys.* **19**, 4317–4329 (2017).
- ¹⁰³A. Nowak, O. Legeza, and K. Boguslawski, "Orbital entanglement and correlation from pCCD-tailored coupled cluster wave functions," *J. Chem. Phys.* **154**, 084111 (2021).
- ¹⁰⁴K. Kowalski and P. Piecuch, "A comparison of the renormalized and active-space coupled-cluster methods: Potential energy curves of BH and F_2 ," *Chem. Phys. Lett.* **344**, 165–175 (2001).
- ¹⁰⁵K. A. Peterson, R. A. Kendall, and T. H. Dunning, "Benchmark Calculations With Correlated Molecular Wave Functions. III. Configuration Interaction Calculations On First Row Homonuclear Diatomics," *J. Chem. Phys.* **99**, 9790–9805 (1993).
- ¹⁰⁶K. P. Huber and G. Herzberg, *Molecular Spectra and Molecular Structure, Vol. IV, Constants of Diatomic Molecules* (Van Nostrand, 1979).
- ¹⁰⁷T. Shimanouchi, H. Matsuura, Y. Ogawa, and I. Harada, "Tables of molecular vibrational frequencies," *J. Phys. Chem. Ref. Data* **7**, 1323–1444 (1978).
- ¹⁰⁸K. K. Irikura, "Experimental vibrational zero-point energies: Diatomic molecules," *J. Phys. Chem. Ref. Data* **36**, 389–397 (2007).
- ¹⁰⁹C. M. Marian, U. Wahlgren, O. Gropen, and P. Pyykkö, "Bonding and electronic structure in diatomic ThO: quasirelativistic effective core potential calculations," *J. Mol. Struct. THEOCHEM* **169**, 339–354 (1988).
- ¹¹⁰J. Paulovic, T. Nakajima, K. Hirao, and L. Seijo, "Relativistic correlating basis sets for the sixth-period d-block atoms from Lu to Hg," *J. Chem. Phys.* **117**, 3597 (2002).
- ¹¹¹E. R. Meyer and J. L. Bohn, "Prospects for an electron electric-dipole moment search in metastable ThO and ThF^+ ," *Phys. Rev. A* **78**, 010502 (2008).
- ¹¹²T. Fleig and M. K. Nayak, "Electron electric dipole moment and hyperfine interaction constants for ThO," *J. Mol. Spec.* **300**, 16–21 (2014).
- ¹¹³L. V. Skripnikov and A. Titov, "Theoretical study of thorium monoxide for the electron electric dipole moment search: Electronic properties of $\text{H}^3\delta_1$ in ThO," *J. Chem. Phys.* **142**, 024301 (2015).

- ¹¹⁴L. V. Skripnikov, "Combined 4-component and relativistic pseudopotential study of the electron electric dipole moment search," *J. Chem. Phys.* **145**, 214301 (2016).
- ¹¹⁵M. Denis and T. Fleig, "In search of discrete symmetry violations beyond the standard model: Thorium monoxide reloaded," *J. Chem. Phys.* **145**, 214307 (2016).
- ¹¹⁶B. Liang and L. Andrews, "Matrix infrared spectra and quasirelativistic DFT studies of ThS and ThS₂," *J. Phys. Chem. A* **106**, 4038–4509 (2002).
- ¹¹⁷M. C. Heaven, B. J. Barker, and I. O. Antonov, "Spectroscopy and structure of the simplest actinide bonds," *Phys. Rev. A* **118**, 10867–10881 (2014).
- ¹¹⁸F. Wang, A. Le, T. C. Steimle, and M. C. Heaven, "Communication: The permanent electric dipole moment of thorium monoxide, ThO," *J. Chem. Phys.* **134**, 031102 (2011).
- ¹¹⁹T. A. C. J. Baron, W. C. Campbell, D. DeMille, J. M. Doyle, G. Gabrielse, Y. V. Gurevich, P. W. Hess, N. R. Hutzler, E. Kirilov, I. Kozyryev, B. R. O'Leary, C. D. Panda, M. F. Parsons, E. S. Petrik, B. Spaun, A. C. Vutha, and A. D. West, "Order of Magnitude Smaller Limit on the Electric Dipole Moment of the Electron," *Science* **343**, 269 (2014).
- ¹²⁰A. Le, M. C. Heaven, and T. C. Steimle, "The permanent electric dipole moment of thorium sulfide, ThS," *J. Chem. Phys.* **140**, 024307 (2014).
- ¹²¹W. R. Wadt, "Why UO₂²⁺ Is Linear and Isoelectronic ThO₂ Is Bent," *J. Am. Chem. Soc.* **103**, 6053–6057 (1981).
- ¹²²K. Dyall, "Bonding and bending in the actinyls," *Mol. Phys.* **96**, 511 (1999).
- ¹²³W. A. de Jong, L. Visscher, and W. C. Nieuwpoort, "On the bonding and the electric field gradient of the uranyl ion," *J. Mol. Struct. THEOCHEM* **458**, 41 (1999).
- ¹²⁴Z. Zhang and R. M. Pitzer, "Application of Relativistic Quantum Chemistry to the Electronic Energy Levels of the Uranyl Ion," *J. Phys. Chem. A* **103**, 6880 (1999).
- ¹²⁵N. Kaltsoyannis, "Computational Study of Analogues of the Uranyl Ion Containing the -NUN- Unit: Density Functional Theory Calculations on UO₂²⁺, UON⁺, UN₂, UO(NPH₃)³⁺, U(NPH₃)₂⁴⁺, [UCl₄NPR₃] (R = H, Me), and [UOCl₄NP(C₆H₅)₃]," *Inorg. Chem.* **39**, 6009–6017 (2000).
- ¹²⁶S. Matsika, Z. Zhang, S. R. Brozell, J.-P. Blaudeau, Q. Wang, and R. M. Pitzer, "Electronic Structure and Spectra of Actinyl Ions," *J. Phys. Chem. A* **105**, 3825–3828 (2001).
- ¹²⁷F. Réal, V. Vallet, C. Marian, and U. Wahlgren, "Theoretical investigation of the energies and geometries of photoexcited uranyl(VI) ion: A comparison between wave-function theory and density functional theory," *J. Phys. Chem.* **127**, 214302 (2007).
- ¹²⁸P. Tecmer, A. S. P. Gomes, U. Ekström, and L. Visscher, "Electronic spectroscopy of UO₂²⁺, NUO⁺ and NUN: an evaluation of time-dependent density functional theory for actinides," *Phys. Chem. Chem. Phys.* **13**, 6249–6259 (2011).
- ¹²⁹F. Wei, G. Wu, W. H. E. Schwarz, and J. Li, "Geometries, electronic structures, and excited states of UN₂, NUO⁺, and UO₂²⁺: a combined CCSD(T), RAS/CASPT2 and TDDFT study," *Theor. Chem. Acc.* **129**, 467 (2011).
- ¹³⁰P. Tecmer, R. Bast, K. Ruud, and L. Visscher, "Charge-Transfer Excitations in Uranyl Tetrachloride ([UO₂Cl₄]²⁻): How Reliable are Electronic Spectra from Relativistic Time-Dependent Density Functional Theory?" *J. Phys. Chem. A* **116**, 7397–7404 (2012).
- ¹³¹P. Tecmer, H. van Lingen, A. S. P. Gomes, and L. Visscher, "The electronic spectrum of CUONg₄ (Ng = Ne, Ar, Kr, Xe): New insights in the interaction of the CUO molecule with noble gas matrices," *J. Chem. Phys.* **137**, 084308 (2012).
- ¹³²P. Tecmer, N. Govind, K. Kowalski, W. A. de Jong, and L. Visscher, "Reliable Modeling of the Electronic Spectra of Realistic Uranium Complexes," *J. Chem. Phys.* **139**, 034301 (2013).
- ¹³³A. S. P. Gomes, F. Réal, B. Schimmelpfennig, U. Wahlgren, and V. Vallet, "Applied computational actinide chemistry," in *Computational Methods in Lanthanide and Actinide Chemistry* (John Wiley & Sons Ltd, Chichester, 2015) Chap. 11, pp. 269–298.
- ¹³⁴A. S. P. Gomes, C. R. Jacob, and L. Visscher, "Calculation of local excitations in large systems by embedding wave-function theory in density-functional theory," *Phys. Chem. Chem. Phys.* **10**, 5353–5362 (2008).
- ¹³⁵P. Tecmer, S. W. Hong, and K. Boguslawski, "Dissecting the cation-ation interaction between two uranyl units," *Phys. Chem. Chem. Phys.* **18**, 18305–18311 (2016).
- ¹³⁶R. Denning, "Electronic Structure and Bonding in Actinyl Ions and their Analogs," *J. Phys. Chem. A* **111**, 4125–4143 (2007).
- ¹³⁷R. Baker, "New reactivity of the uranyl(VI) ion," *Chem. Eur. J.* **18**, 16258–16271 (2012).
- ¹³⁸C. Clavaguéra-Sarrio, N. Ismail, C. J. Marsden, D. Bégue, and C. Pouchan, "Calculation of harmonic and anharmonic vibrational wavenumbers for triatomic uranium compounds XUY," *Chem. Phys.* **302**, 1–11 (2004).
- ¹³⁹K. Pierloot and E. van Besien, "Electronic structure and spectrum of UO₂²⁺ and UO₂Cl₄²⁻," *J. Phys. Chem.* **123**, 204309 (2005).
- ¹⁴⁰R. D. Hunt, J. T. Yustein, and L. Andrews, "Matrix infrared-spectra of NUN formed by the insertion of uranium atoms into molecular nitrogen," *J. Chem. Phys.* **98**, 6070 (1993).
- ¹⁴¹A. Kovács, R.J.M. Konings, "Computed vibrational frequencies of actinide oxides AnO^{0/+ /2+} and AnO₂^{0/+ /2+} (An = Th, Pa, U, Np, Pu, Am, Cm)," *J. Phys. Chem. A* **115**, 6646–6656 (2011).
- ¹⁴²A. Kovács, R. J. M. Konings, J. K. Gibson, I. Infante, and L. Gagliardi, "Quantum chemical calculations and experimental investigations of molecular actinide oxides," *Chem. Rev.* **115**, 1725–1759 (2015).
- ¹⁴³K. Boguslawski, "Targeting Doubly Excited States with Equation of Motion Coupled Cluster Theory Restricted to Double Excitations," *J. Chem. Theory Comput.* **15**, 18–24 (2019).
- ¹⁴⁴K. Kowalski and P. Piecuch, "New coupled-cluster methods with singles, doubles, and noniterative triples for high accuracy calculations of excited electronic states," *J. Chem. Phys.* **120**, 1715–1738 (2004).